Computer Applications to Geotechnical Problems in Highway Engineering

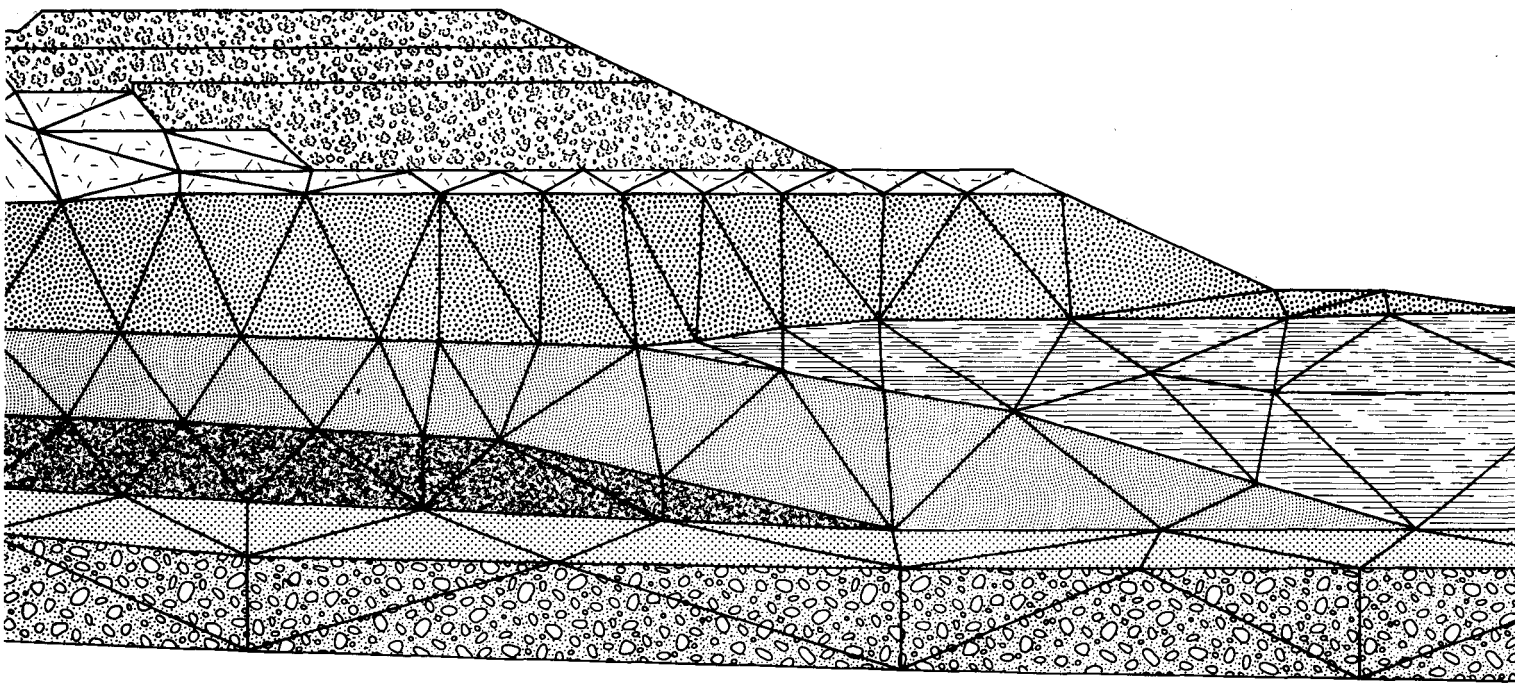

Cambridge 1980

The Symposium was sponsored by the Department of Transport, Highway Engineering Computer Branch, organised by PM Geotechnical Analysts Ltd under the direction of the organising committee, with the co-operation of the Soil Mechanics Group, Cambridge University Engineering Department.

Editor

M F Randolph

Published by PM Geotechnical Analysts Ltd

Cambridge 1981

FINITE ELEMENT ANALYSES OF WALLS, FOOTINGS AND SLOPES

D V GRIFFITHS*

SUMMARY

The paper describes some viscoplastic iterative solutions to classical problems of soil mechanics.

Solutions for von Mises materials are shown to be straightforward in their application, but frictional materials, and especially cohesionless soils require more complex yield surfaces and carefully considered initial stress conditions. The paper discusses some of the conical yield criteria available for use with sands and some of the convergence difficulties that may be encountered.

The viscoplastic approach is shown to enable simple implementation of strain softening phenomena for both clays and sands and some aspects of undrained behaviour are also discussed.

INTRODUCTION

The aim of this paper is to indicate some of the potentials and shortcomings of using elasto-plastic models to simulate the collapse behaviour of soil. More specifically, elastic-perfectly plastic materials are assumed to behave as linear elastic solids until the stress conditions are such that some yield condition is violated. At this point plastic flow occurs resulting in irrecoverable strains being generated according to some plastic flow rule.

The behaviour of frictionless materials such as undrained clays ($\phi_u = 0$) with respect to total stresses can be examined using the familiar von Mises failure criterion. For soils possessing both cohesion and friction the more general Mohr Coulomb yield criterion is applicable. For $\phi_u = 0$ soils, Mohr Coulomb reduces to Tresca's criterion which gives similar results to von Mises.

Incorrect volume change and stress paths prior to and at collapse are valid criticisms of the simple elasto-plastic models, but in drained problems this is not a serious handicap. Zienkiewicz et al (1975) showed that only in undrained or highly confined problems did the volume change (and hence the potential surface assumed) affect collapse loads significantly. Objections to Mohr Coulomb type yield surfaces on account of the corners these surfaces possess in principal stress space led to a variety of right circular cones being suggested by various workers as approximations to Mohr Coulomb. The problems of corners is easily overcome in the present work using a method suggested by Zienkiewicz and Cormeau (1974) and in any case the conical yield surfaces have been shown by Bishop (1966) to not adequately represent soil strength under general 3-D stress states.

---

* University of Manchester

Mohr Coulomb's yield criterion has stood the test of time well and is still used as a basis for teaching and design in soil mechanics. Strictly speaking, of course, Mohr Coulomb's yield surface is 'wrong' as it completely disregards the influence of the intermediate principal stress σ_2. Attempts to allow for the influence of σ_2 have been made in soil analysis by adjusting the friction angle rather than tampering with the yield criterion itself leading to some ambiguity regarding what ϕ value to use in a given analysis (Ko and Scott, 1973). Some workers have postulated yield criteria for soils which are appropriate to general stress states, but the advantages gained over Mohr Coulomb do not seem to justify the added complexity of their formulation for drained analyses.

The examples discussed in the following sections have used a Mohr Coulomb yield criterion in conjunction with a plane strain analysis. The ϕ value used in these cases is therefore assumed to be that measured in a plane strain test. If ϕ_c as measured in triaxial compression is used (as is often the case in design) conservative solutions will always be obtained as it is well known that $\phi_{ps} > \phi_c$.

The Finite Element formulation uses viscoplastic theory, and this has been shown (Zienkiewicz and Cormeau, 1972, 1974) to be an efficient and versatile way of incorporating different yield criteria and plastic potentials. For a given system of external and body forces acting on a soil mass, the method iterates using equivalent elastic solutions until both equilibrium and yield conditions are satisfied which for a Mohr Coulomb material requires that

$$\frac{\partial \sigma_x}{\partial x} + \frac{\partial \tau_{xy}}{\partial y} = 0$$

$$\frac{\partial \sigma_y}{\partial y} + \frac{\partial \tau_{xy}}{\partial x} = \gamma \qquad (1)$$

$$(\sigma_y - \sigma_x)^2 + 4\tau_{xy}^2 = (\sigma_x + \sigma_y + 2c\cot\phi)^2 \sin^2\phi$$

If these equations could be satisfied exactly the solution would be a statically admissible solution and hence a lower bound. Although equilibrium is always satisifed in the Finite Element formulation, the convergence criterion is such that yield conditions are always violated by a small amount when computation ceases. This numerical hardening may be controlled by adjusting the tolerances, but has not proved to be a serious problem.

All the Finite Element solutions described in this report used 8-node quadrilateral elements and 'reduced' 2 × 2 point integration.

SIMPLE YIELD CRITERIA

Figures 1 and 2 show π-plane representations of some of the better known yield criteria available to approximate soil strength. The yield surfaces are all given by $F = 0$ where F is given as a function of soil strength parameters and the current stresses. The yield function compares the shear stresses with the shear strength of the soil. If $F < 0$ elastic behaviour is assumed, and visco-plastic behaviour occurs if $F \geq 0$. The stresses are conveniently expressed in terms of 3 independent stress invariants where in plane strain

$$\sigma_m = \frac{\sigma_x + \sigma_y + \sigma_z}{3}$$

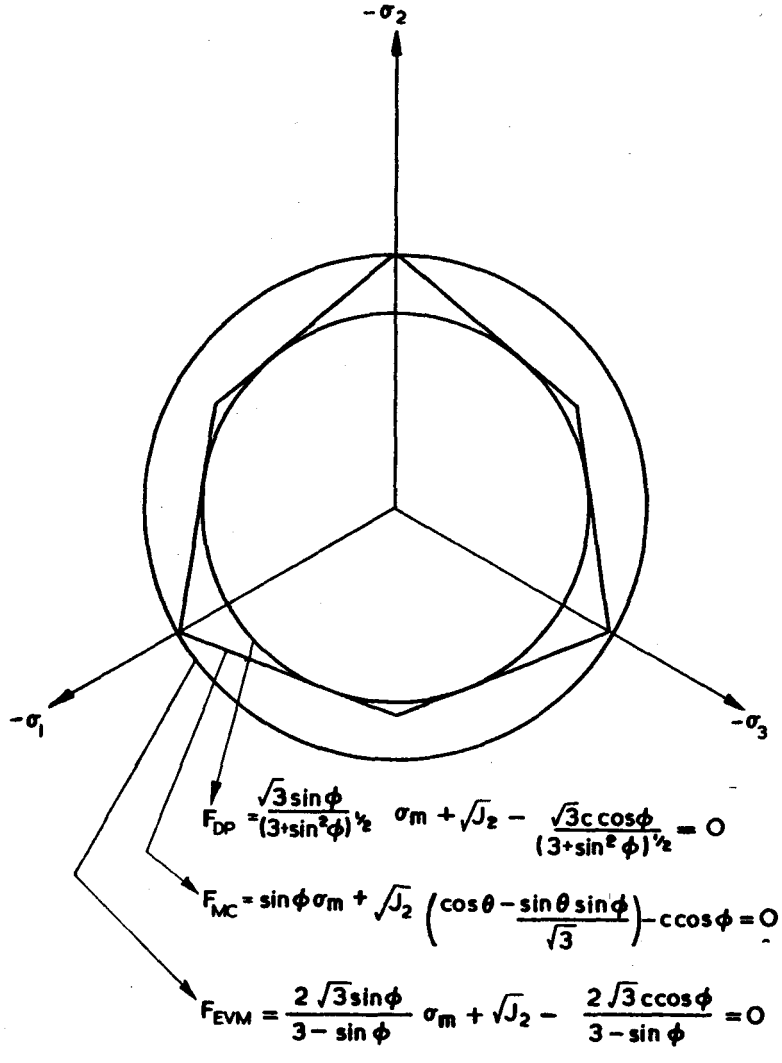

CONICAL YIELD CRITERIA FIG. 1.

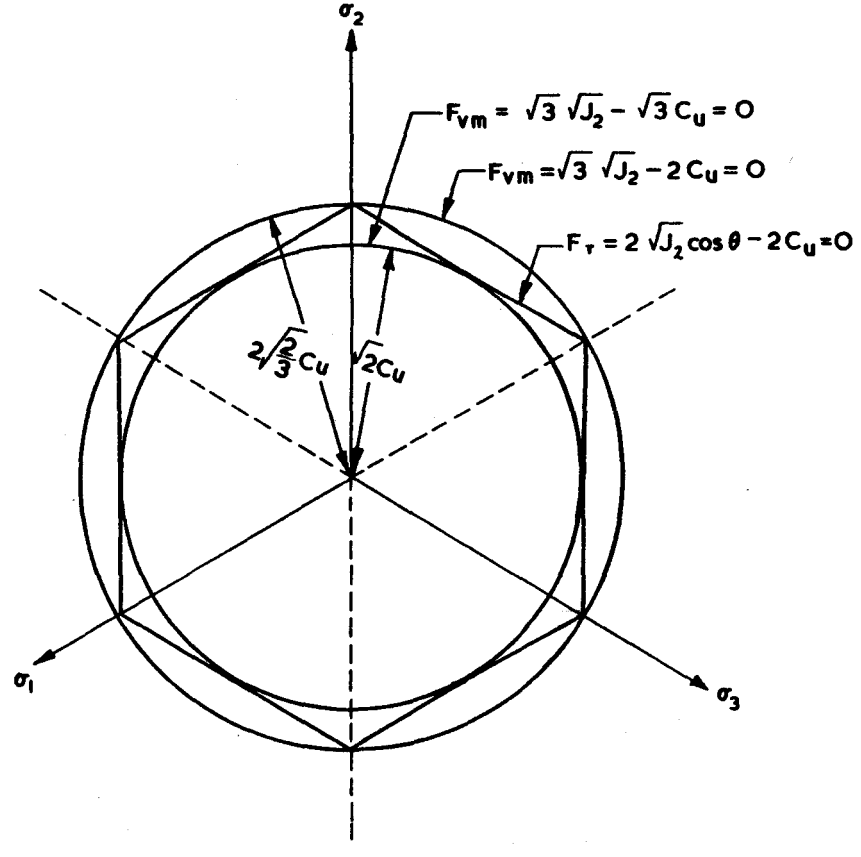

VON MISES AND TRESCA YIELD SURFACES FIG. 2

$$J_2 = \tfrac{1}{6}[(\sigma_x - \sigma_y)^2 + (\sigma_y - \sigma_z)^2 + (\sigma_z - \sigma_x)^2 + 6\tau_{xy}^2] \quad (2)$$

$$\theta = \tfrac{1}{3}\arcsin\left(\frac{-3\sqrt{3}\,J_2}{2J_2^{3/2}}\right)$$

where

$$J_3 = S_x S_y S_z - S_z \tau_{xy}^2$$

and $$S_x = \frac{2\sigma_x - \sigma_y - \sigma_z}{3}$$

$\sqrt{3}\,\sigma_m$ defines a particular π plane and $\sqrt{2}\,\sqrt{J_2}$ and θ act as radial coordinates within that plane. It should be remembered that any yield surface with a circular projection in the π plane will be independent of θ, and any cylindrical surface will be independent of confining pressure σ_m.

Figure 3 shows the shortcomings of the right circular cones when applied to general stress states, and the Extended von Mises surface in particular predicts enormous strength in triaxial extension as the friction angle increases. Mohr Coulomb's surface predicts the same stress ratio at failure in extension and compression and will be slightly conservative as experimental evidence (Lade, 1972) suggests slightly greater strengths in extension.

Strain softening or "brittle" soil behaviour may be modelled by modifying the yield surfaces after peak strength has been reached. In the case of a $\phi_u = 0$ material the radius of von Mises cylinder may be reduced to a value corresponding to c_{RES} once c_{PEAK} has been mobilised. Altering the size of a yield surface during yield presents no computational difficulties in viscoplasticity and also gives a simple physical interpretation of softening in principal stress space.

EARTH PRESSURE COMPUTATIONS

The Finite Element mesh used for earth pressure computations is shown in Fig. 4. The wall was assumed to be perfectly smooth and stresses were applied to the soil mass by translating the wall horizontally. Stresses on the wall were obtained at the Gauss points adjacent to it (other wall roughnesses were considered, but the data will not be presented here).

Figures 5 and 6 show the limiting active and passive forces computed for a $\phi_u = 0$ and a $c = 0$ soil using von Mises' and Mohr Coulomb's yield criteria respectively. The solutions agree well with Rankine's classical smooth wall solutions. In the case of the frictional soil, the well known difference between strain to failure in the passive and active cases is reproduced. Figures 7 and 8 show the limiting stress distribution computed at passive collapse.

Figures 9 and 10 give the displacement vectors and yielding zone at collapse for a general $c - \phi$ soil. It should be noted that analysis of a soil as a weightless material is possible provided cohesion is present. Analysis of a cohesionless material however, must always include self weight otherwise the soil has zero strength irrespective of ϕ. In all cases considered here, initial conditions of $K_o = 1$ were assumed. Making K_o other than unity did not affect collapse

	Extension stress ratio	Compression stress ratio	V
VM	$\frac{3+\sin\phi}{3-5\sin\phi}$	$\tan^2\left(45+\frac{\phi}{2}\right)$	$1+\frac{4\sin^2\phi}{3-2\sin\phi-5\sin^2\phi}$
DP	$\frac{(3+\sin^2\phi)^{1/2}+\sin\phi}{(3+\sin^2\phi)^{1/2}-2\sin\phi}$	$\frac{(3+\sin^2\phi)^{1/2}+2\sin\phi}{(3+\sin^2\phi)^{1/2}-\sin\phi}$	$\frac{1}{1-\sin^2\phi}$
MC	$\tan^2\left(45+\frac{\phi}{2}\right)$	$\tan^2\left(45+\frac{\phi}{2}\right)$	1

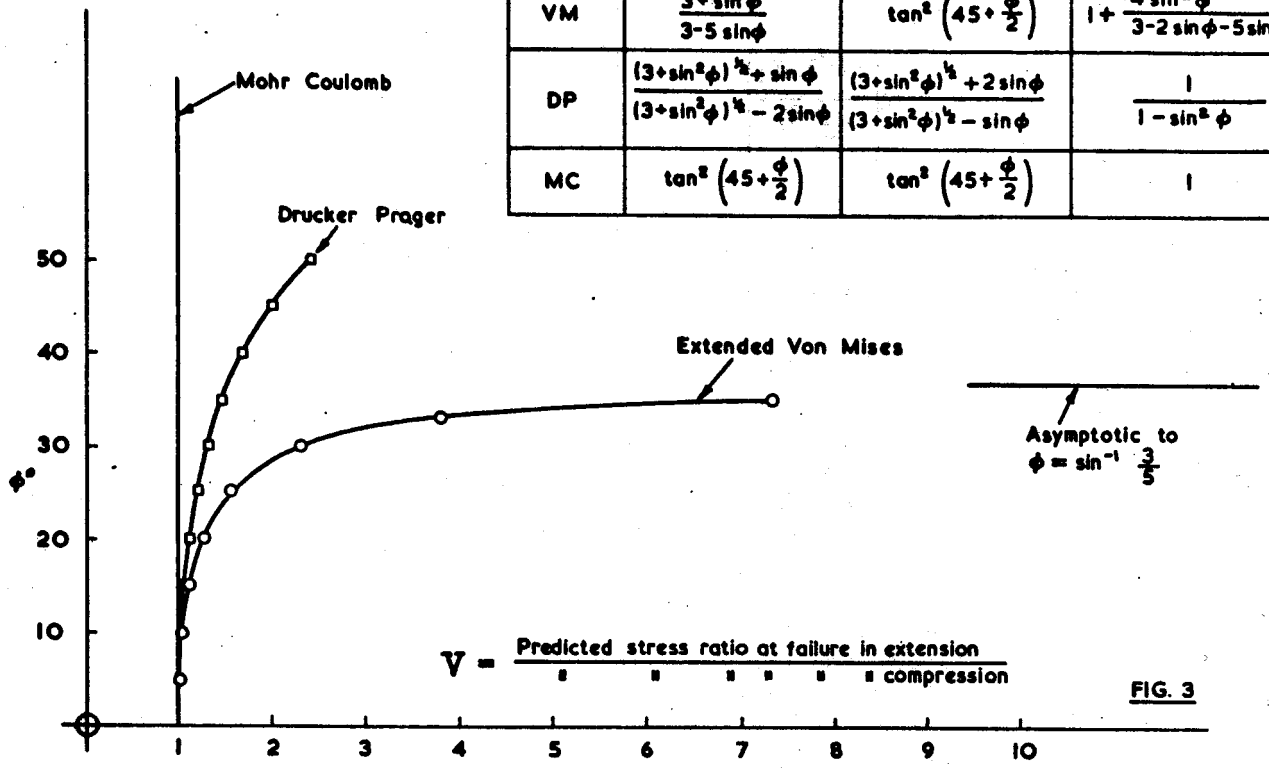

FIG. 3

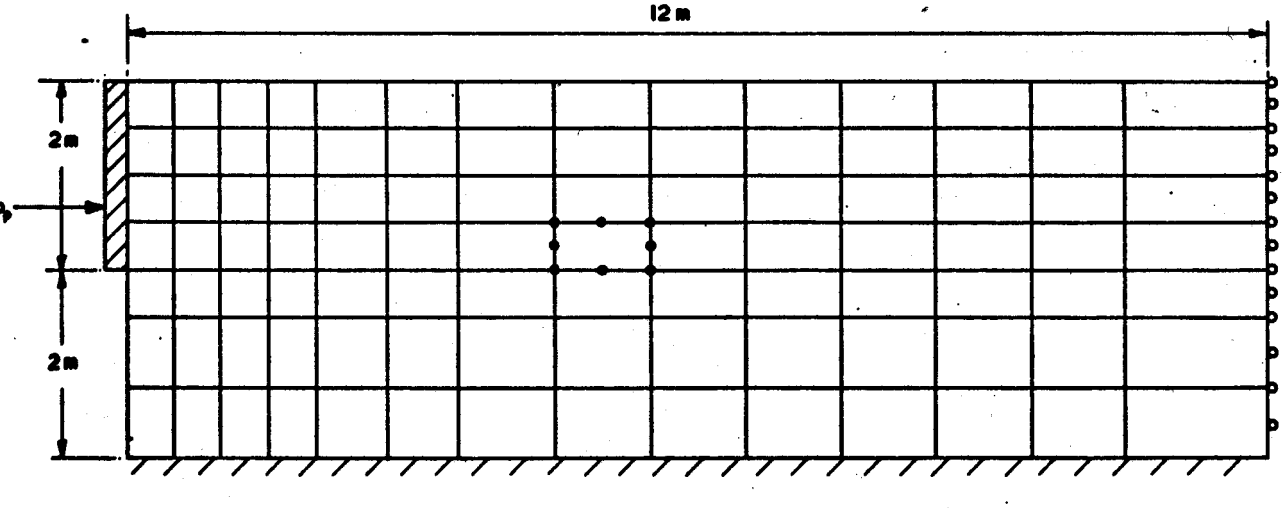

MESH USED FOR EARTH PRESSURE COMPUTATION

FIG. 4

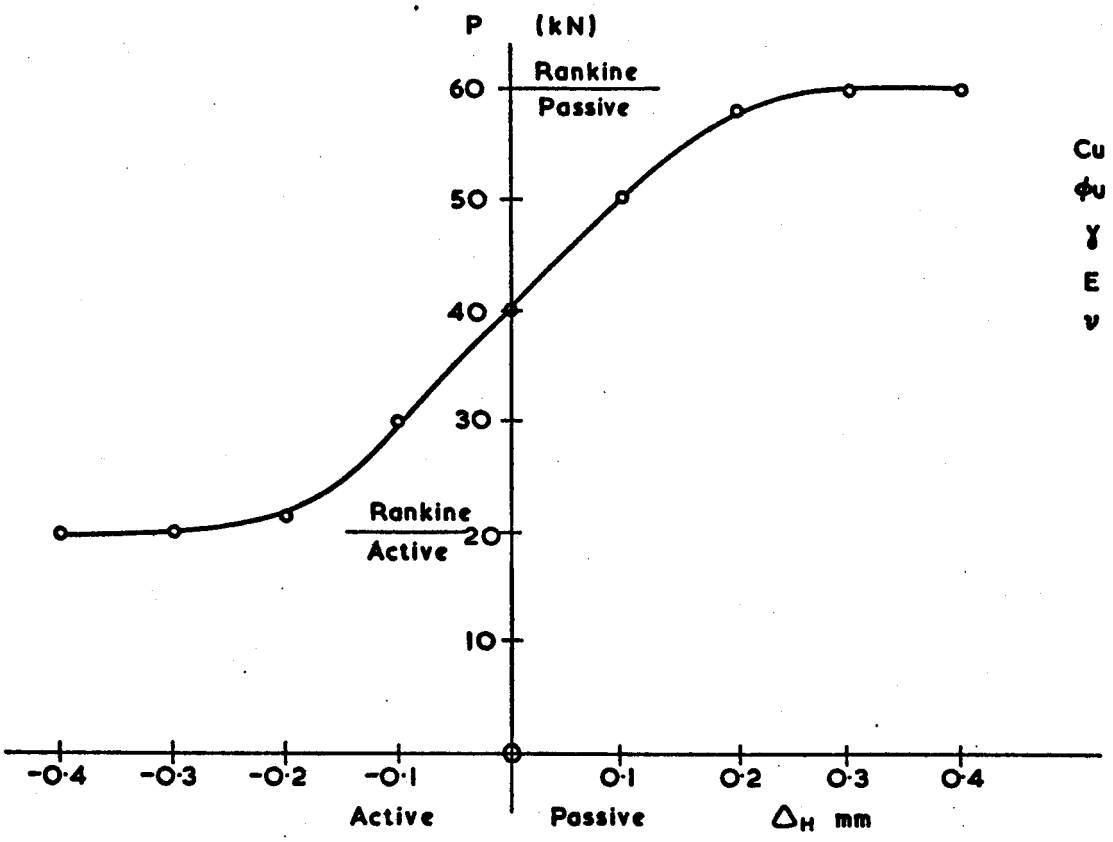

ACTIVE AND PASSIVE LIMIT STATES.

FIG. 5

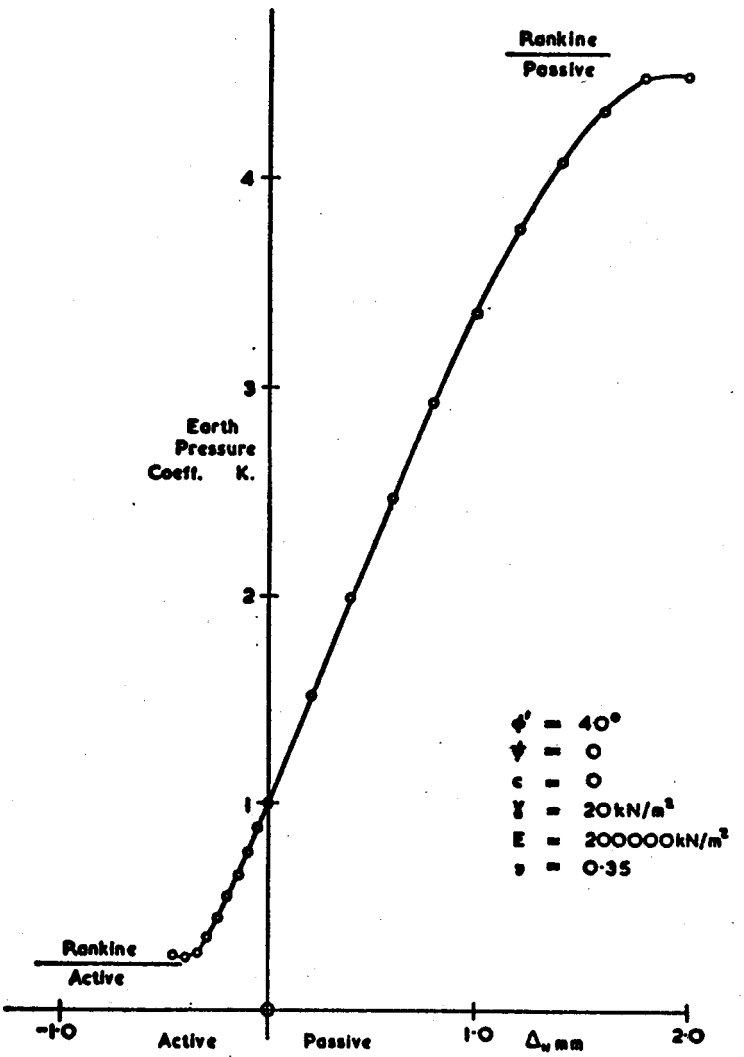

PASSIVE AND ACTIVE LIMIT STATES

FIG. 6

loads, but merely the strains required to generate collapse.

The value of Young's modulus incorporated into the elastic portion of the model also had the effect of scaling displacements but did not influence the collapse loads. Accurate predictions of displacements prior to collapse require more sophisticated stress dependent elastic moduli as suggested by Duncan and Chang (1970).

Simple strain softening behaviour was incorporated into both the cohesive and the frictional soil models (Figs. 11 and 12). For the cohesive material, softening was obtained by reducing the radius of von Mises cylinder as a function of equivalent total strain to a minimum radius of $\sqrt{2}\ C_{RES}$. From Fig. 11 it can be seen that a quite sudden drop in wall load is computed as softening comes into effect. The peak mobilised cohesion C_m lies between C_{PEAK} and C_{RES} as expected, and the more brittle the stress-strain law the closer is peak C_m to C_{RES}. In principle any function of $\bar{\sigma}$ vs $\bar{\varepsilon}$ may be used as the stress-strain law for a von Mises material due to yield being governed by one invariant only. Present work on continuously yielding materials will be the subject of a later paper.

Any compatible pair of stress and strain invariants may be used in a von Mises stress-strain law. In this paper the definitions are

$$\bar{\sigma} = \sqrt{3}\sqrt{J_2} = \frac{1}{\sqrt{2}}\left[(\sigma_x - \sigma_y)^2 + (\sigma_y - \sigma_z)^2 + (\sigma_z - \sigma_x)^2 + 6\tau_{xy}^2\right]^{\frac{1}{2}}$$

and $$\bar{\varepsilon} = \frac{\sqrt{2}}{3}\left[(\varepsilon_x - \varepsilon_y)^2 + (\varepsilon_y - \varepsilon_z)^2 + (\varepsilon_z - \varepsilon_x)^2 + \tfrac{3}{2}\gamma_{xy}^2\right]^{\frac{1}{2}} \qquad (3)$$

$$\left(\frac{\bar{\sigma}}{\bar{\varepsilon}}\right)_{elastic} = 3G$$

where

$$G = \frac{E}{2(1 + \nu)}$$

For the frictional model an explicit strain softening law is difficult to formulate on account of yield being governed by all three stress invariants. The strain at which different portions of the soil mass first reach yield varies considerably depending on the initial stress state and elastic stress path inside the yield surface. The simple model in Fig. 12 incorporates a switch from peak ϕ to residual once peak stress ratio has been reached. Naturally a smoother transition to residual strength would be more realistic, but the passive resistance computed is in agreement with the general findings of Rowe and Peaker (1965), that it is unconservative to compute passive resistance using a Rankine analysis with ϕ_{PEAK} and the actual ϕ for design lies somewhere between ϕ_{PEAK} and ϕ_{RES} due to progressive failure. This is also true in the active state, and if small enough increments of wall displacement are prescribed, the active force is seen to fall and then rise slightly (Fig. 13) due to the increase in K_A as ϕ drops to its residual value.

In all the cases discussed in this section convergence of results was obtained without difficulty, and computer time was not a serious problem. Generally speaking the greater the ϕ value used in an analysis, the more iterations required to converge. For example, the results quoted in Fig. 6 used a

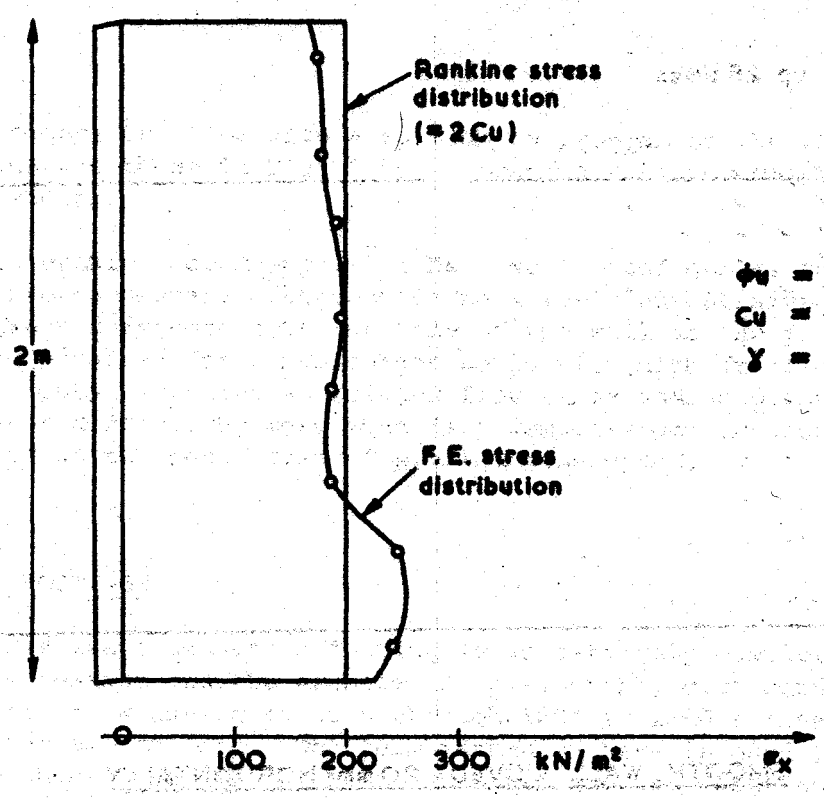

ϕ_u = 0
Cu = 100 kN/m²
γ = 0 (weightless)

PRESSURE DISTRIBUTION OF WEIGHTLESS FRICTIONLESS SOIL ON PASSIVE SHEARLESS WALL

FIG. 7

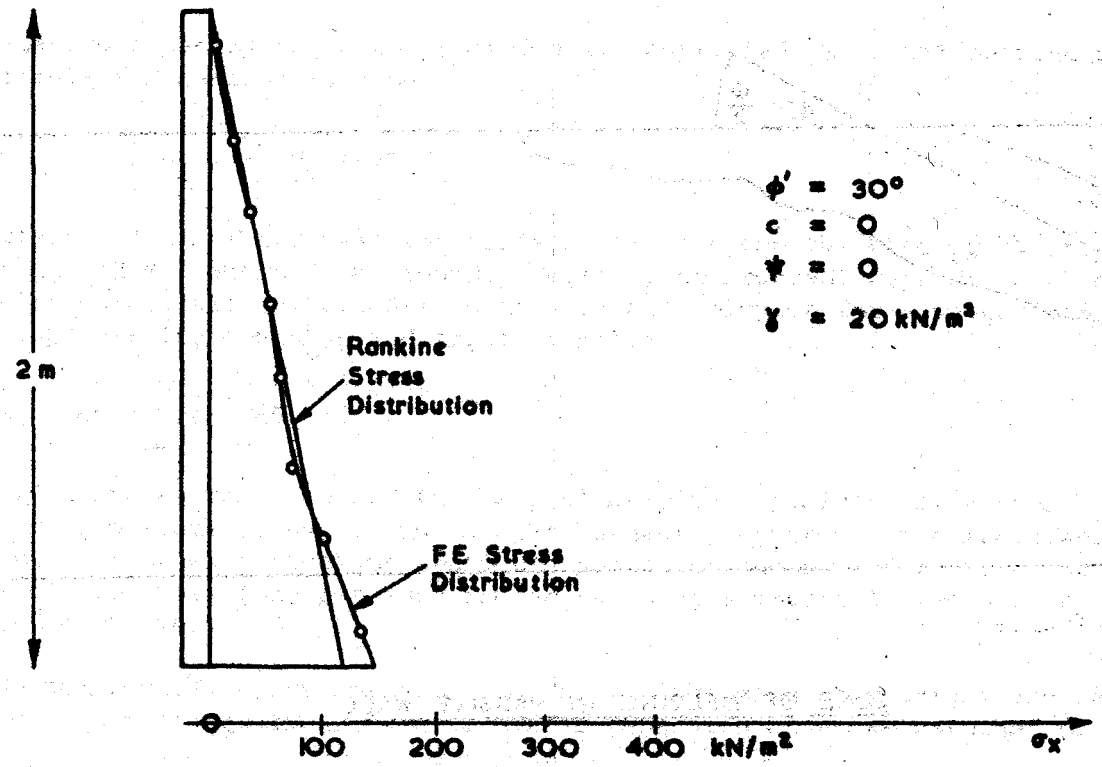

ϕ' = 30°
c = 0
ψ = 0
γ = 20 kN/m³

PRESSURE DISTRIBUTION OF COHESIONLESS SOIL ON PASSIVE SHEARLESS WALL

FIG. 8

Displacements scaled up 25 times

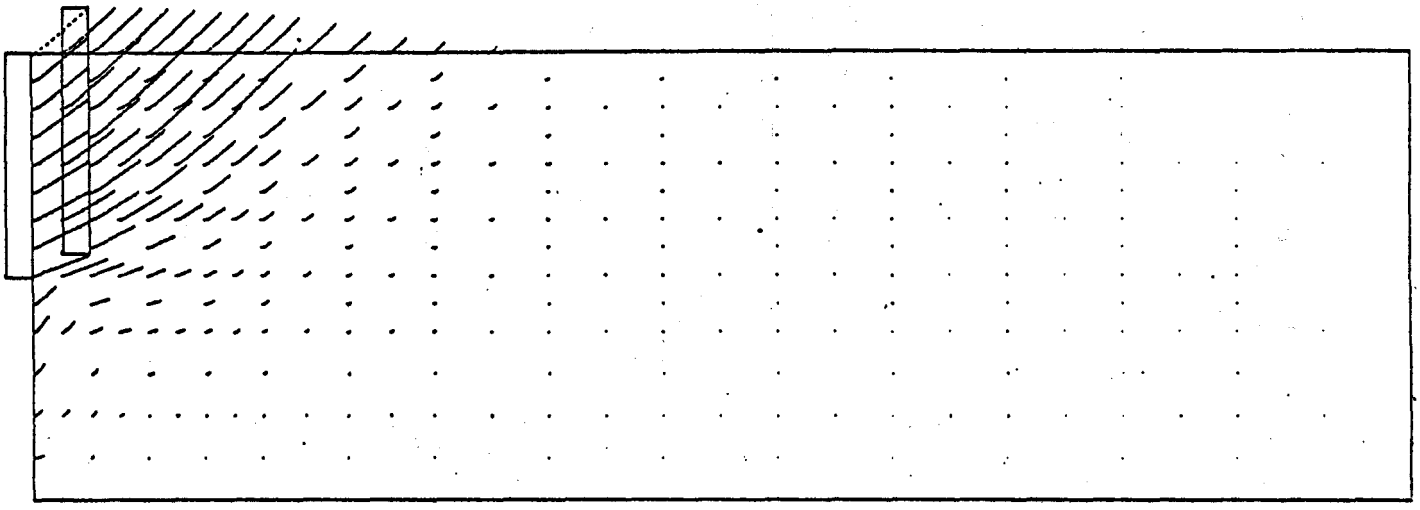

ELASTO PLASTIC
$E = 207000\ kN/m^2$
$\nu = 0.3$
$\phi = 30 \quad \psi = 0$
$c = 20\ kN/m^2$

SMOOTH WALL MOVED 20 mm HORIZONTALLY

FIG. 9.

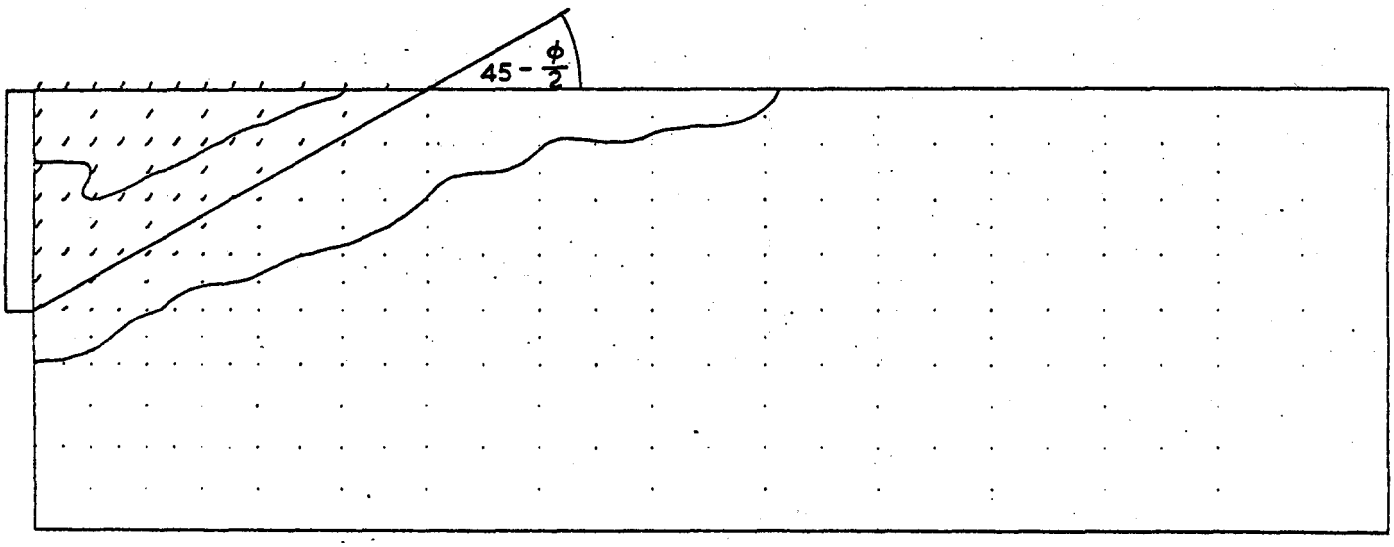

$\phi = 30 \cdot \quad \psi = 0$
$c = 20\ kN/m^2$

ZONE OF YIELDING IN PASSIVE WALL

FIG. 10

total of 90 seconds CPU time with a Fortran IV program on the CDC 7600 at Manchester, whereas those in Fig. 5 corresponding to a von Mises material required 15 seconds.

The wall problem would appear to be a well posed one as far as plasticity calculations are concerned. The mesh is relatively unrestrained, and the plastic flow can progress unimpeded from the base of the wall to the free surface. Solutions were obtained for cohesionless soils with high friction angles and the collapse loads obtained using associated flow rules and no plastic volume change flow rules never differed by more than 3%. Computations are considerably less straightforward in the next class of problem considered.

SURFACE STRIP FOOTINGS

The stress state beneath a footing is an extremely complex one. Active and passive states coexist and the problem is considerably more confined than the wall with the plastic flow having to turn through 180° to find a free surface and permit a 'mechanism' to form. The term mechanism here is used to mean a region of soil whose shear strength has been exhausted and can offer no more resistance to movement.

A natural starting point for any footing analysis is Prandtl's problem of a smooth rigid footing pushed into a cohesive soil. The results of such an analysis using a von Mises yield criterion are presented in Fig. 14.

Unlike the wall problem, convergence became noticeably harder to achieve as the friction angle was increased to $\phi > 30°$. Convergence of some footing problems required hundreds of iterations if allowed and correspondingly high computer times. Convergence problems became even worse if associated flow rules were used even though the bearing capacities computed were not much higher.

Bearing capacity has been traditionally estimated using the bearing capacity formula for shallow footings

$$q_{ULT} = c\, N_c + \frac{\gamma B}{2} N_\gamma + \gamma D\, N_q \qquad (4)$$

If we disregard the third term for surface footings the two bearing capacity factors N_c and N_γ remain to be found. There is no argument over N_c which has been obtained theoretically by Prandtl in his 'exact' solution for a weightless material possessing cohesion and friction where

$$N_c = \cot\phi \left[\tan^2\left(45 + \frac{\phi}{2}\right) e^{\pi \tan\phi} - 1 \right] \qquad (5)$$

Figure 15 compares computed and theoretical bearing capacities of a smooth rigid footing on a weightless soil. The slight hardening apparent as ϕ increases is due to the convergence problems mentioned above and the necessity to allow a maximum of 100 iterations per load increment using a critical time step as described by Cormeau (1975).

No theoretical solutions exist for soils including self weight and hence the second term of equation (4) will differ depending on whose value of N_γ is used.

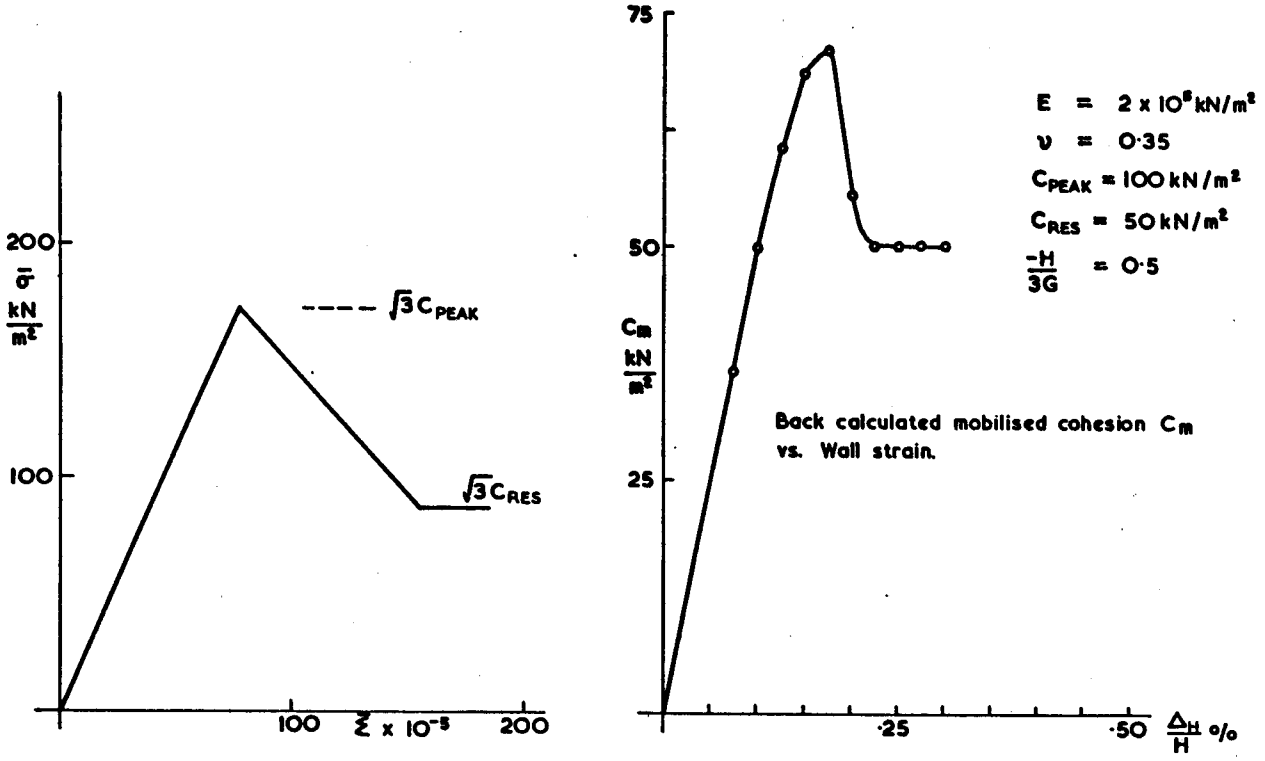

STRAIN SOFTENING COHESIVE SOIL

FIG. 11.

STRAIN SOFTENING FRICTIONAL SOIL.

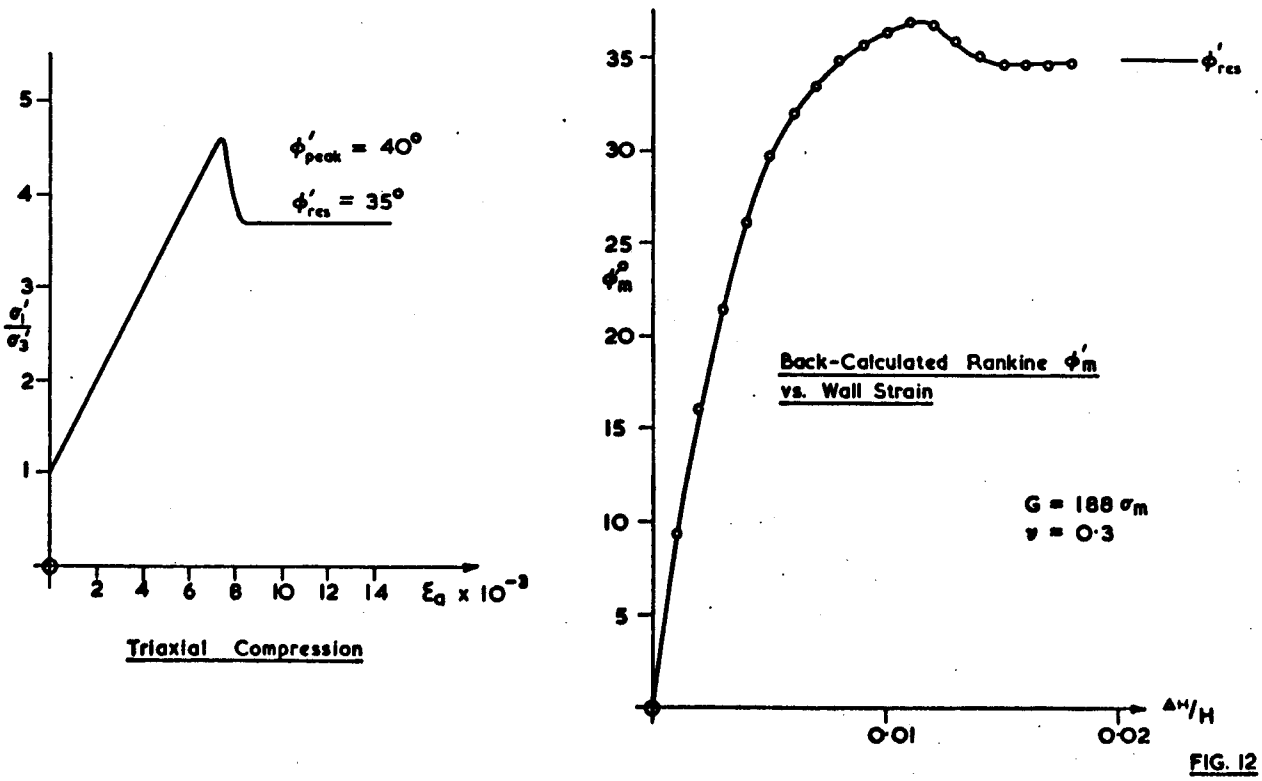

FIG. 12

Figure 16 shows the displacement vectors at collapse of a footing on a soil possessing self weight. The N_γ value back-calcuated from the computed value is compared with that of various workers in Table 1.

TABLE 1

Soil Properties	$\phi = 25°$ $c = 5$ kN/m^2 $\gamma = 20$ kN/m^3	Width B = 2.5 m $N_c = 20.7$
Name	N_γ	q_{ULT} (kN/m^2)
Meyerhof	6.74	272
B Hansen	6.76	273
Sokolovsky	6.92	277
Hill type	7.16	283
Computed	8.70	321
Terzaghi	($N_c = 24$) 9.80	365
Prandtl/Caquot	14.32	461

It is seen that the N_γ value varies by over 100% between that of Meyerhof and of Prandtl/Caquot. In general the greater the contribution to bearing capacity due to the c N_c term the closer will be the computed result to those predicted by classical approaches. Figure 17 compares computed results for a smooth rigid footing of width 2.5 m on a ponderable soil of cohesion 20 kN/m^2 with a variety of other formulae.

A brief analysis of bearing capacity was performed using stress control. This enabled a check to be made on the displacement pattern of a perfectly flexible footing on different soil types. Figure 18 shows such displacements beneath a footing on soils with and without frictional components of strength. Collapse in each case was signalled by a sudden increase in displacements and iterations when the ultimate stress level was reached. (Collapse stresses obtained by this approach were always within a few percent of those predicted by averaging stresses beneath a footing under displacement control.)

Computed displacements were greatest at the centreline of a flexible footing on a $\phi_u = 0$ soil, but for the frictional soil, displacements were greatest towards the footing edge. This result would appear to give some credence to the suggestion in some texts that walls "lean out" on sandy foundations and "lean in" when the foundation rests on undrained clay.

The same softening model as suggested in Figure 11 was incorporated in the footing problem with a von Mises yield criterion. From the jagged shape of Fig.

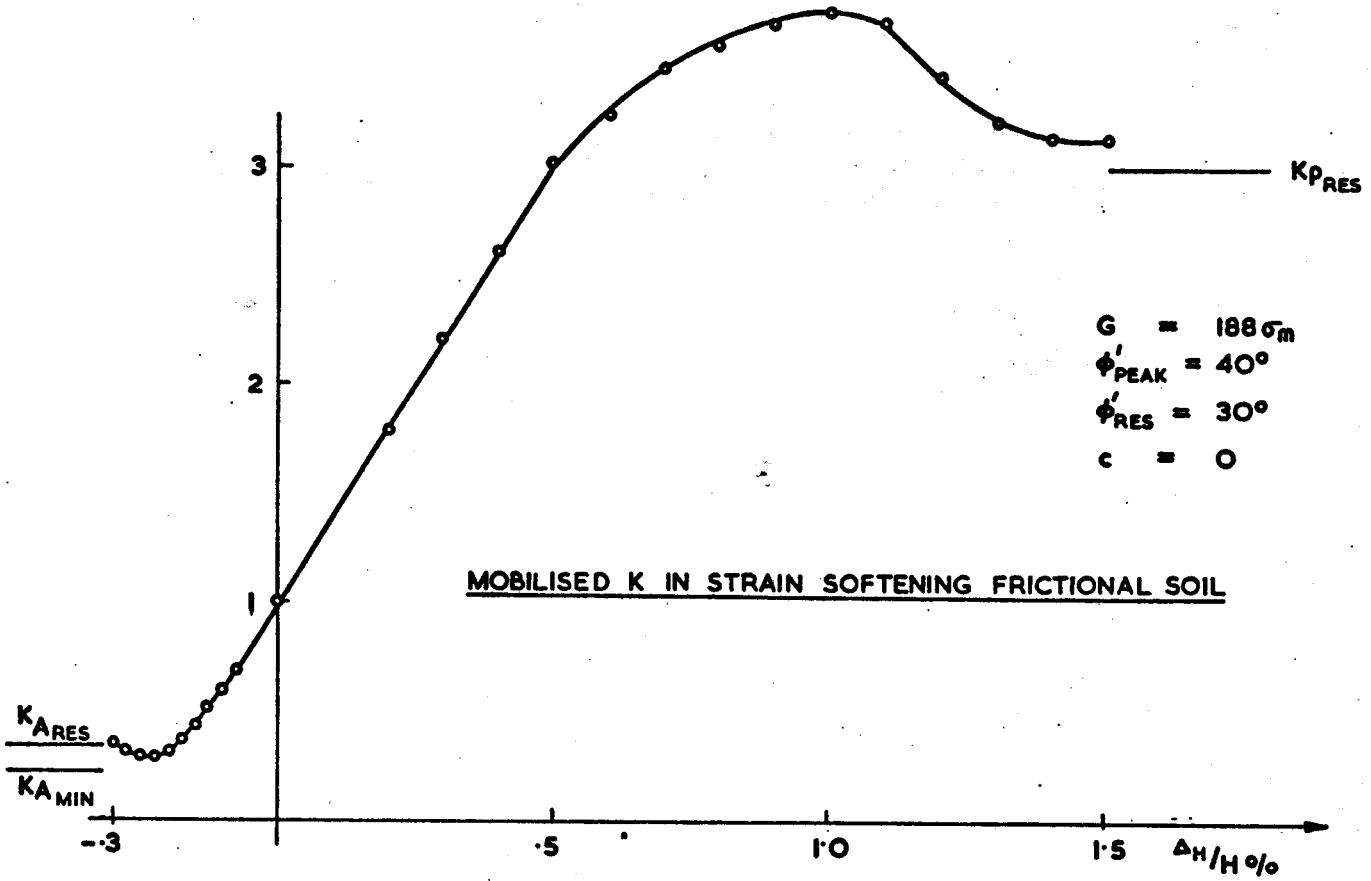

MOBILISED K IN STRAIN SOFTENING FRICTIONAL SOIL

FIG. 13

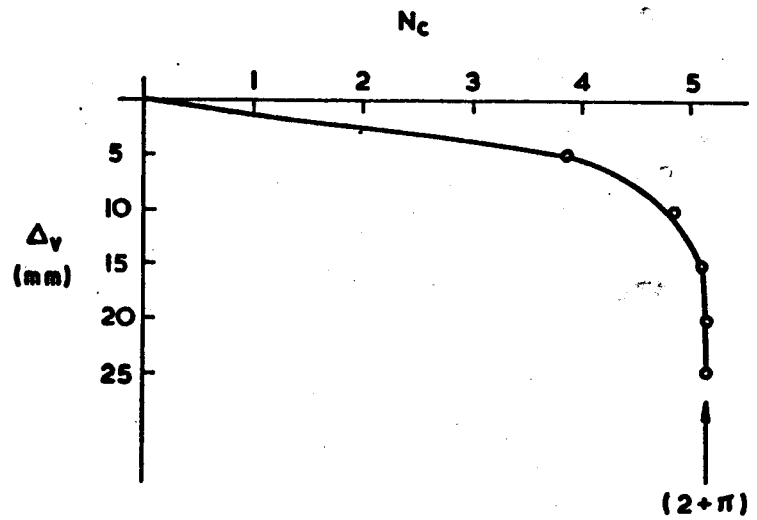

E = 2 x 10^5 kN/m^2
ν = 0·3

RIGID SMOOTH FOOTING ON COHESIVE SOIL

FIG. 14

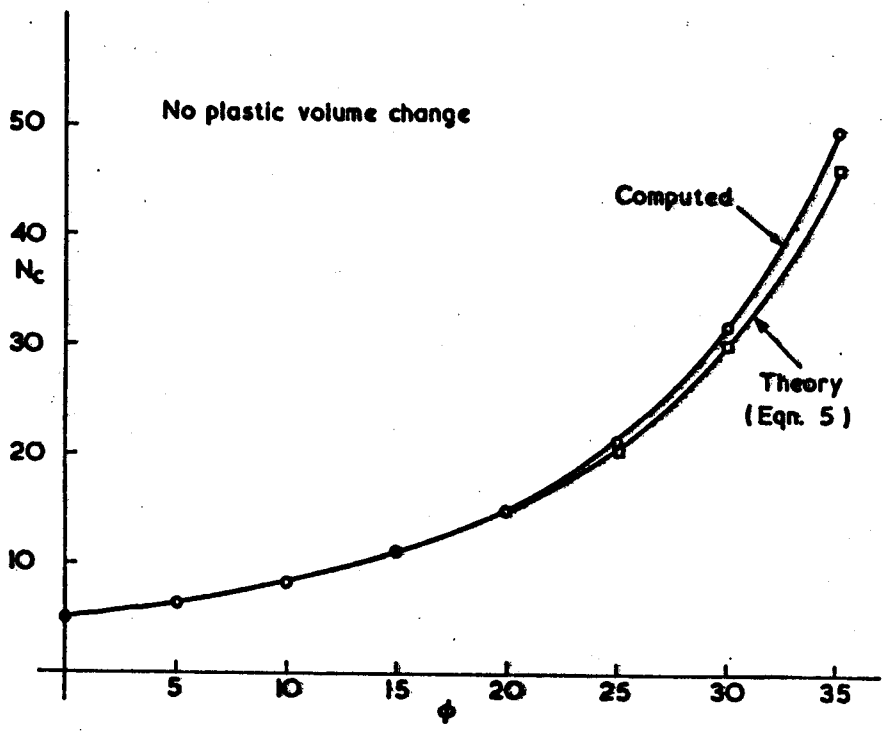

COMPUTED VALUES OF N_c FOR SMOOTH STRIP FOOTING.

FIG. 15

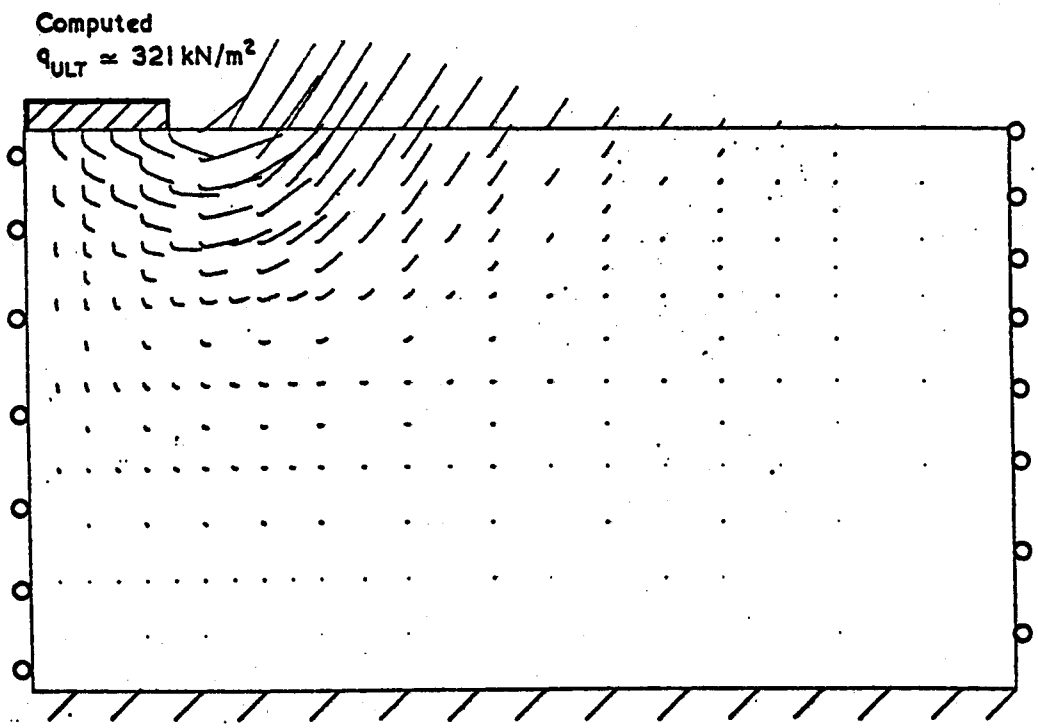

$\phi = \psi = 25°$
$c = 5\ kN/m^2$
$\gamma = 20\ kN/m^3$
$B = 2{\cdot}5\ m$
$K_o = 1$

FAILURE OF RIGID FOOTING.

FIG. 16.

19 it can be seen that progressive failure occurs under a footing in a much less ordered fashion than with the passive wall. The unstable region between first yield and residual values would appear to be due to the complex stress state beneath the footing being forced to follow the stress-strain law of Fig. 11 by the numerical process. It was found that less brittle stress-strain behaviour resulted in smoothing of this transitional zone.

DEEP STRIP FOUNDATIONS

The bearing capacity factors referred to in the previous section are applicable only to 'shallow' foundations and become highly conservative for high D/B. Finite Element calculations have been performed on a number of meshes whose D/B ratios range from 1 to 12, and a typical mesh is given in Fig. 20. To make boundary conditions as simple as possible, bearing pressure was applied to the deep strip in the form of prescribed displacements at the foundation level.

The first type of soil considered was a weightless undrained clay using a Tresca yield criterion. A decision had to be made as to the boundary conditions along face AB. This face could either be left open or restrained laterally and results for both options are compared with Meyerhof's predictions (Meyerhof, 1951) in Fig. 21. When the face was left open a mechanism of the Meyerhof type could form easily with plastic flow into the 'open' hole (Fig. 22). When the hole was laterally supported 'collapse' in the plastic sense could not occur until yield had spread all the way to the free surface at ground level. The supported hole condition would predict increasingly large q_{ULT} values as D/B was increased whereas the open hole gave a limiting q_{ULT} value of 7.5 c at about D/B = 8 and any further increase in D/B did not result in a larger q_{ULT} value. This latter behaviour is closer to field experience although the N_c value computed is lower than Meyerhof's predicted value of $N_c = (2 + 2\pi) = 8.28$ for a deep strip. The likelihood is that the actual mechanism that occurs in the field lies somewhere between the two extreme boundary value problems analysed here. Plastic flow of the type suggested by Meyerhof is certainly open to doubt if a rigid foundation is preventing the mechanism from developing fully. On the other hand, compressibility of the soil and the footing itself would probably be sufficient to allow some plastic flow to occur between the base and sides of the foundation. It is arguable therefore that the two cases taken for analysis represent upper and lower bounds to the true behaviour.

Using the open hole model, further calculations were performed to obtain the bearing capacity of a weightless soil possessing both cohesion and friction. Here, as with the cohesive material, it was found that bearing pressures levelled out for $D/B \geq 8$ as shown in Fig. 23. The figure indicates that as ϕ increase q_{ULT} increases very rapidly, especially for the deeper footings and a difference of a few degrees in ϕ can alter q_{ULT} considerably. The sensitivity of the value of q_{ULT} to ϕ used in the analysis as ϕ became large was reflected in the numerical process in the form of large numbers of iterations to converge. This was even more apparent when self weight was included in the analysis (Fig. 24) and these results were obtained by allowing a maximum of 100 iterations per displacement increment. This many iterations was always sufficient for small friction angles, but for $\phi > 30$ the algorithm would frequently have used more if allowed. Stopping calculations after an arbitrary number of iterations and not permitting normal convergence inevitably leads to some numerical hardening and overestimation of q_{ULT}.

It is perhaps fortunate that the class of problem which is hardest to solve numerically is also the least interesting physically as far as ultimate conditions

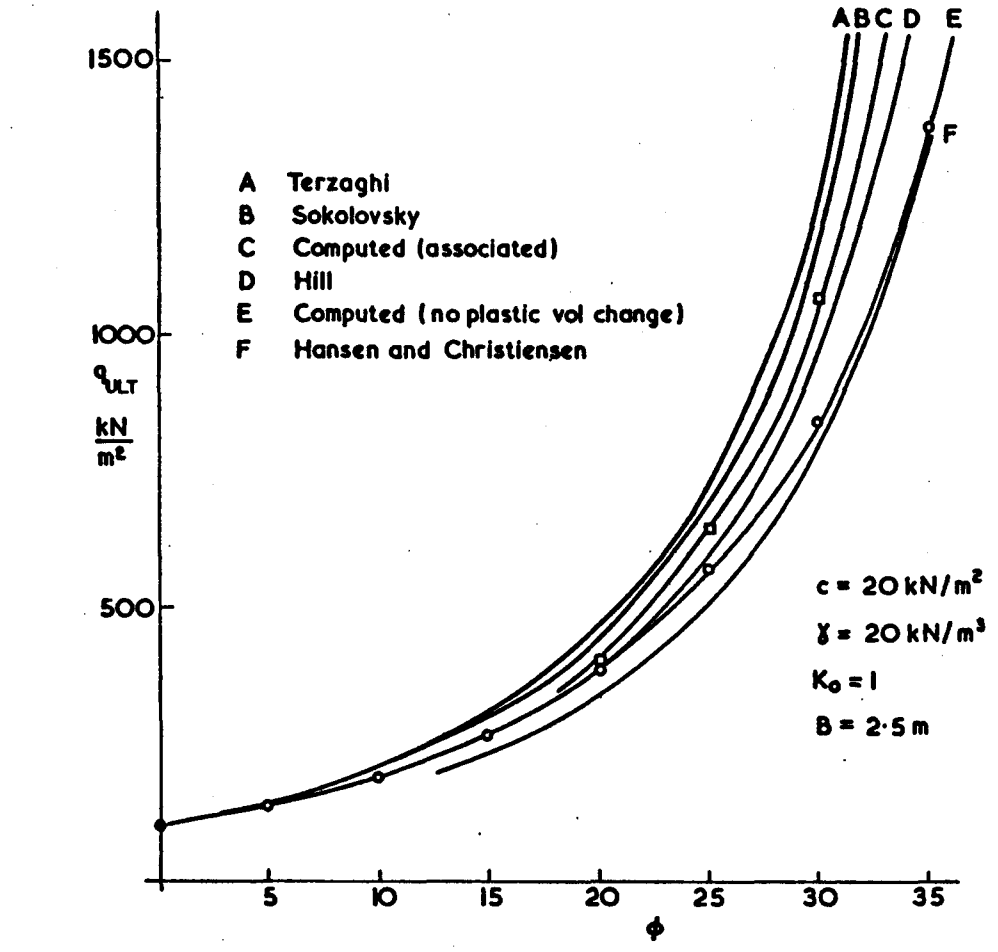

FIG. 17

BEARING CAPACITY OF A SMOOTH RIGID FOOTING.

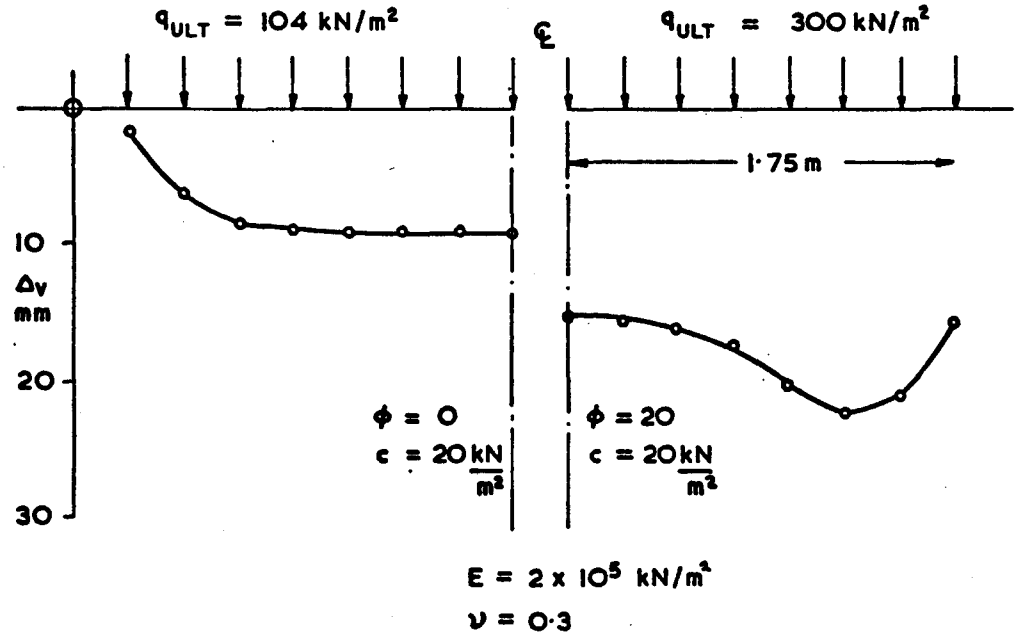

DISPLACEMENTS AT COLLAPSE OF A FLEXIBLE FOOTING UNDER UNIFORM STRESS

FIG. 18

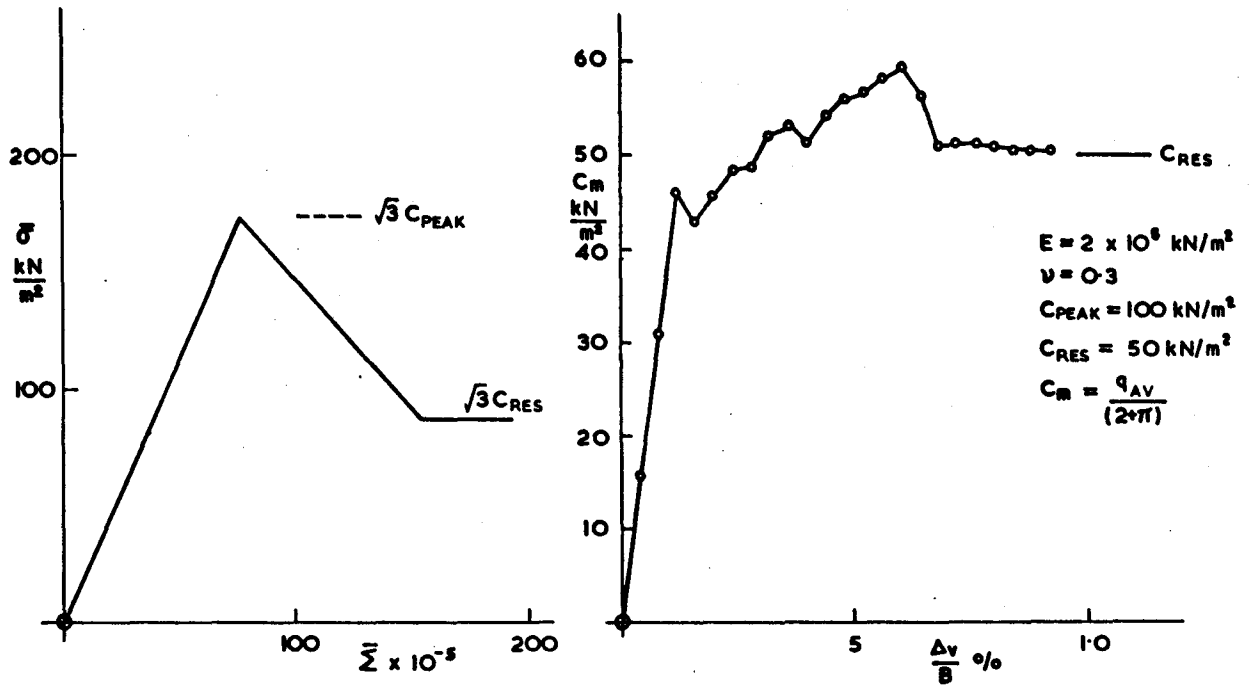

STRAIN SOFTENING COHESIVE SOIL

FIG. 19.

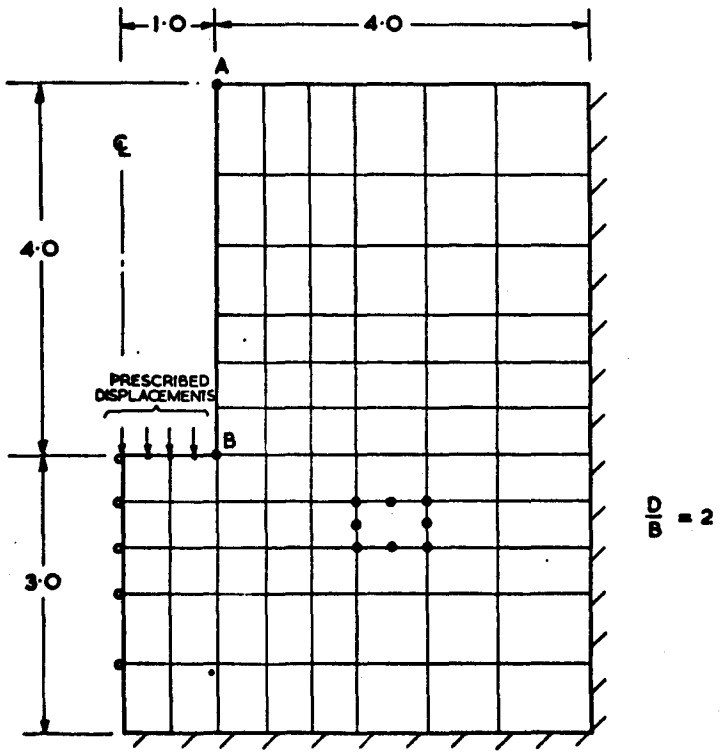

MESH USED FOR ANALYSIS OF DEEP FOUNDATIONS.

FIG. 20

and collapse are concerned. Design of foundations of predominantly frictional soils is rarely governed by collapse considerations. This is because settlements become excessive due to soil compressibility before collapse is reached in all but the narrowest footings.

In real soils at high confining stresses such as those occuring under deep foundations, crushing takes place during shear and this will result in a reduced ϕ value. In principal stress space this would take the form of a curved Mohr Coulomb failure surface where ϕ reduces as a function of σ_m. The simple model used here takes no account of this phenomenon although it could easily be included if empirical data relating ϕ to σ_m were available.

The results given in Figs. 23 and 24 were all obtained using a flow rule of no plastic volume change. Fully associated flow rules invariably gave higher collapse loads due to the added confinement induced by the volume increase, but the difference in q_{ULT} obtained was not significant. The volume change predicted by the associated flow rules however, was at times ridiculously large (Fig. 25).

No analytical solutions exist for deep foundations although Chen (1975) performed upper bound limit analyses using Prandtl and Hill mechanisms. These solutions are in reasonable agreement for shallow footings but are significantly less than those predicted here as D/B is increased. The mechanisms chosen by Chen were different to those observed in the Finite Element calculations which were of the Meyerhof type, although it might be argued that the combination of the boundary restraints and the open hole in the Finite Element mesh conspired to give the soil 'no choice' as to the direction of plastic flow. Further investigations of the elastoplastic behaviour of deep foundations are currently being made.

SLOPE STABILITY

Elastoplastic analyses of slopes using the finite element method have been presented by Smith and Hobbs (1974) for cohesive slopes and by Zienkiewicz et al (1975) for soil possessing both cohesion and friction. It has been shown that by the application of gravity loads (and hence stresses) to a slope with known strength, instability would be indicated by large displacements and slow convergence. A stable slope would converge quickly or even remain elastic. It was suggested that by reducing each of the components of shear strength in turn while keeping the other constant until failure occured, factors of safety on c and $\tan\phi$ could be obtained which would not necessarily be the same.

The example cited here is very similar to that described by Zienkiewicz et al (1975) and the mesh used is given in Fig. 26. Attempts were made to find the shear strength parameters to just cause collapse of the slope under gravity in the cases of a cohesive soil and a general c - ϕ soil.

The effect of reducing c on the vertical deflexion of the crest of the slope is given in Fig. 27a and is in excellent agreement with Taylor's (1937) analytical prediction.

By keeping c constant and reducing ϕ in a general soil gave collapse in close agreement with Bishop and Morgenstern's (1960) effective stress method, Fig. 27b. The plastic displacement vectors at collapse are superimposed in Fig. 28 for both these soils and as expected the frictional soil displays a more shallow failure zone than the cohesive material.

From	D/B	Nc
	1	6
	3	7

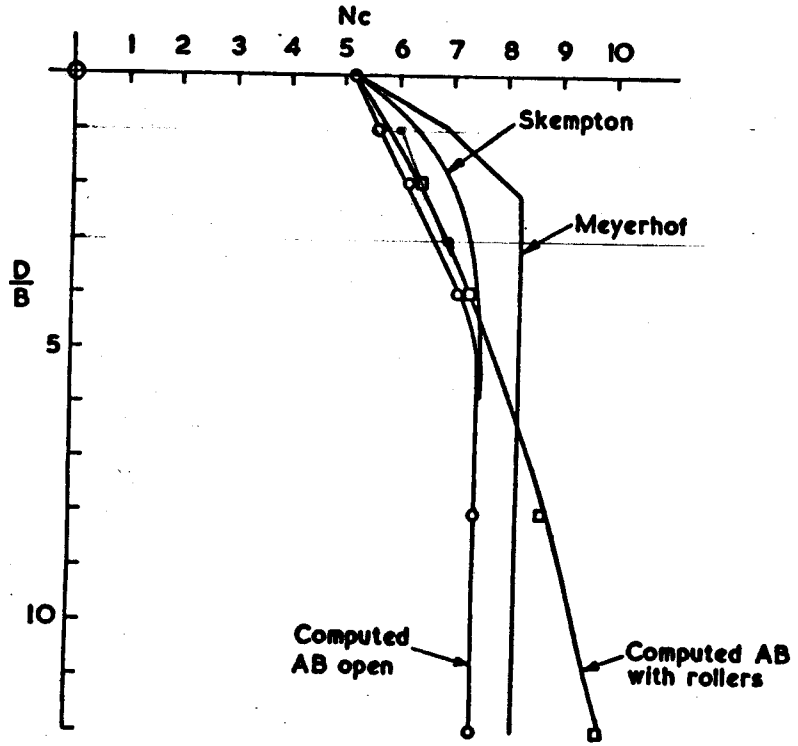

BEARING CAPACITY OF DEEP STRIP IN IDEAL COHESIVE SOIL.

FIG. 21

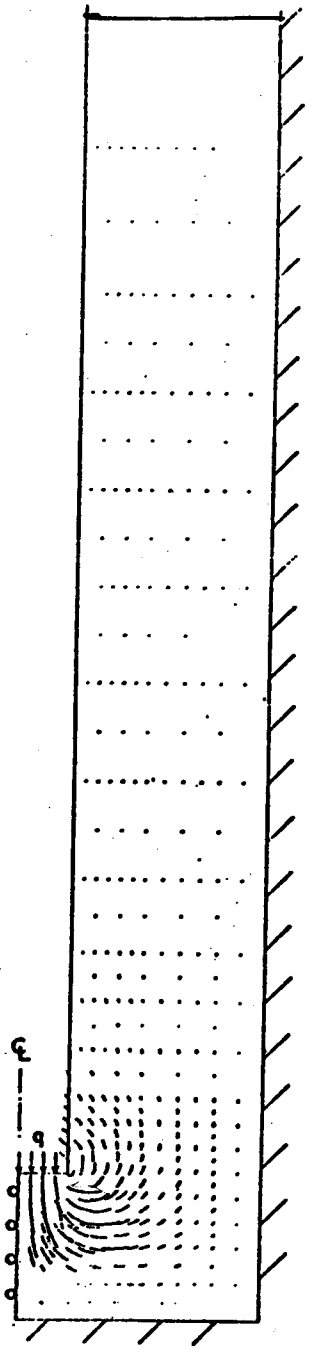

$\frac{D}{B} = 12$

$Cu = 20\ kN/m^2$

$q_{ULT} = 150\ kN/m^2$

COLLAPSE MODE OF DEEP STRIP IN COHESIVE SOIL.

FIG. 22.

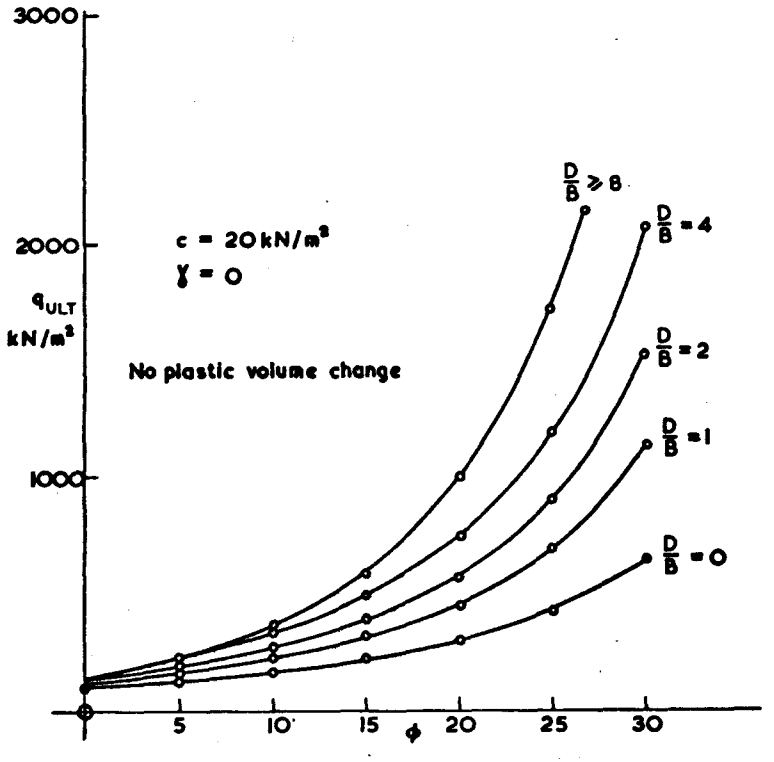

BEARING CAPACITY OF DEEP RIGID STRIP FOUNDATION ON WEIGHTLESS SOIL.

FIG 23

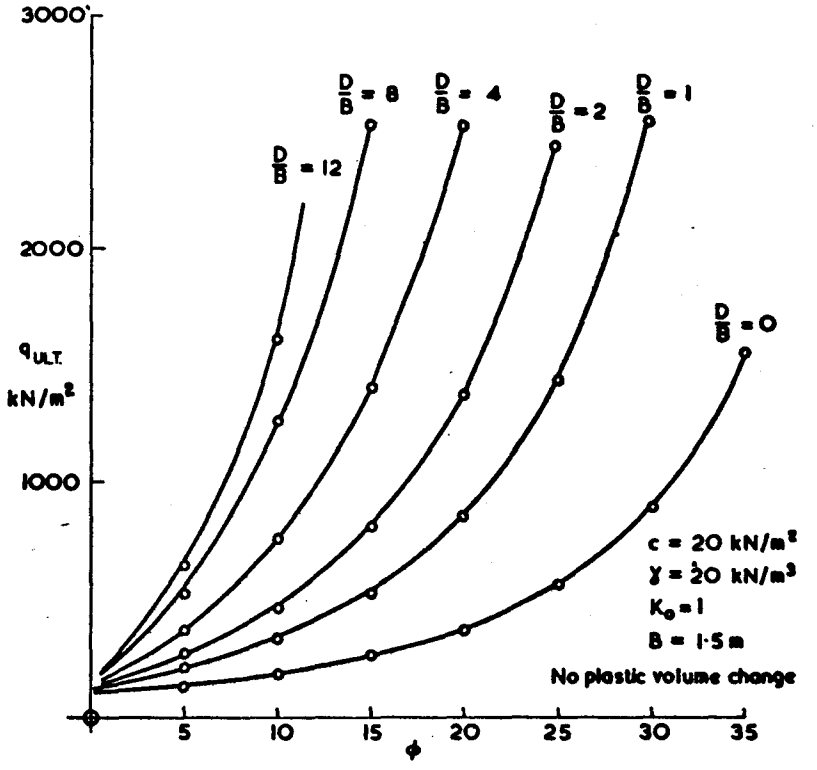

BEARING CAPACITY OF DEEP RIGID STRIP FOUNDATION ON SOIL WITH SELF WEIGHT.

FIG. 24

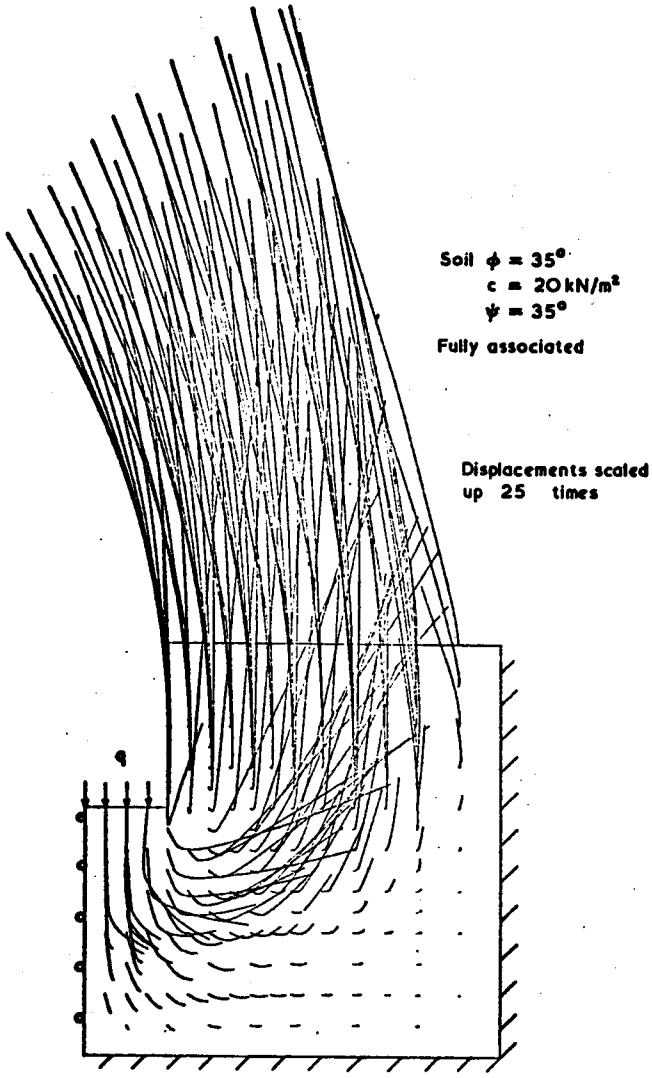

"ASSOCIATED FLOW RULES PREDICT EXCESSIVE DILATION !"

FIG. 25

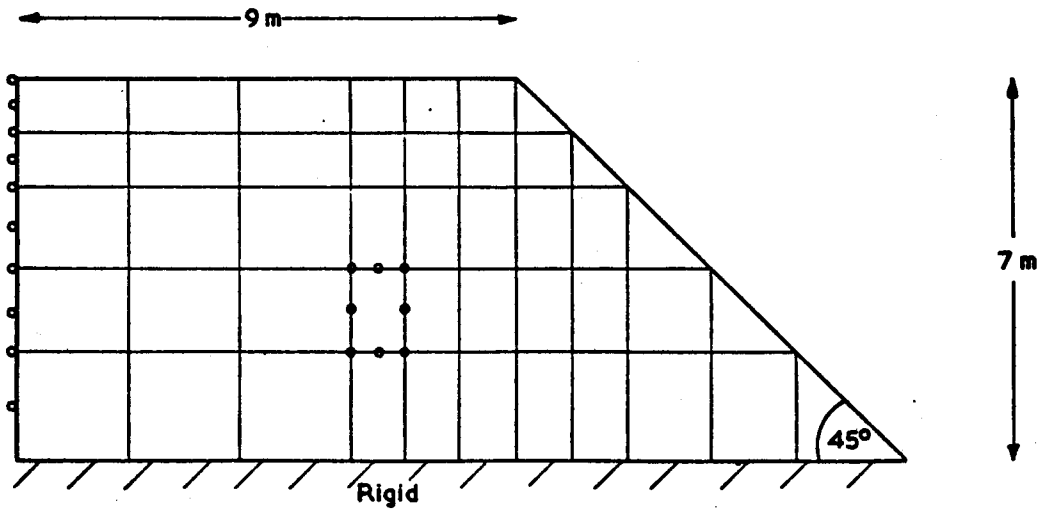

MESH USED FOR ANALYSIS OF SLOPE STABILITY

FIG. 26

UNDRAINED BEHAVIOUR

Accurate numerical modelling of undrained soil behaviour is considerably harder than the drained problems mentioned hitherto. This is due to the important role that volume change plays on the effective stresses and hence strength of the soil. A dilating material in an undrained analysis will become stronger as the pore pressures fall and bind the particles harder together. Failure will not occur until either crushing of the soil results in critical state conditions or the pore fluid cavitates (Seed and Lee, 1967).

The potential surfaces used in the examples given in previous sections are totally inadequate for accurate volume change predictions. Elastic behaviour is assumed inside the yield surface, and this can only result in volume decrease ($\nu < 0.5$). When the stress path touches the yield surface plastic strains occur according to the flow rule. With the exception of using a dilation angle of zero, these plastic strains will always be dilative. The simple model therefore predicts a small volume decrease followed by a dilation which is similar to the behaviour of dense sands under shear, but for the wrong reasons!

Undrained analyses have been performed on the simple model using the method suggested by Naylor (1974) whereby a large fluid stiffness is added into the volumetric parts of the effective soil stiffness matrix. The behaviour of the wall under these conditions is given in Fig. 29 for three different dilation angles. It is seen that only the soil with no plastic volume change can fail in shear, and when the dilation angle is positive the soil appears to have unlimited resources of passive resistance! The results of incorporating a simple cavitation model are shown in Fig. 30. This model assumes that if the water pressure falls to 100 kN/m^2 of tension it stays at that value due to cavitation, and the soil can now reach yield as the mean stresses are no longer rising.

Apart from the inadequate volume change predictions of the simple models, a truly undrained analysis will certainly overestimate the influence of dilation on pore pressure due to the permeability of the soil which may be quite large for granular soils. In this case consolidation and plasticity theories must be coupled (Zienkiewicz et al, 1978).

CONCLUSION

Simple elastoplastic models have been shown to be of value in predicting the collapse loads of typical soil mechanics problems under drained conditions. The majority of examples presented here have been shown to compare well with theoretical solutions and this justifies the use of the method in more complex and realistic problems involving non uniform properties and geometries.

Analysis of footings using these models was straightforward for soils possessing a large cohesive component, but as friction was increased convergence became harder to achieve.

Undrained problems were analysed using the simple model and some features of real soil behaviour can be reproduced but for essentially the wrong reasons. Realistic modelling of undrained behaviour requires more sophisticated flow rules with stress dependent potential surfaces which can cope with both plastic contraction and dilation.

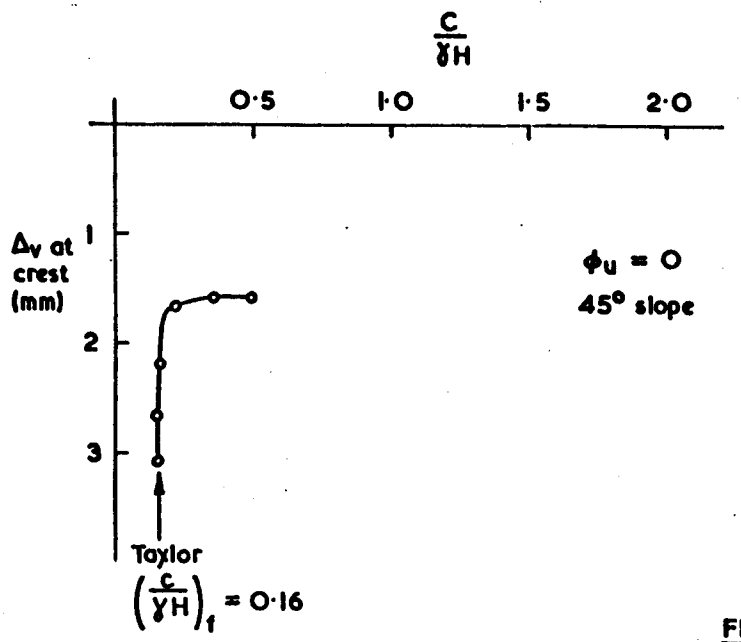

FIG. 27a

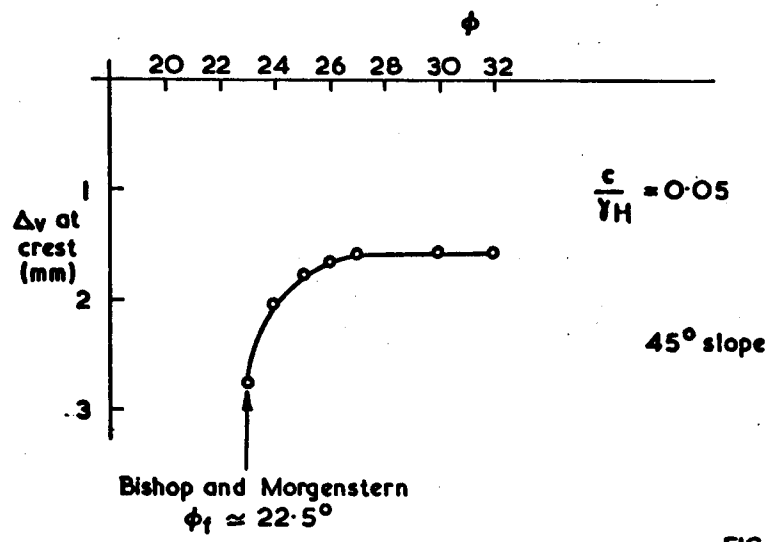

FIG. 27b

VERTICAL CREST DISPLACEMENT

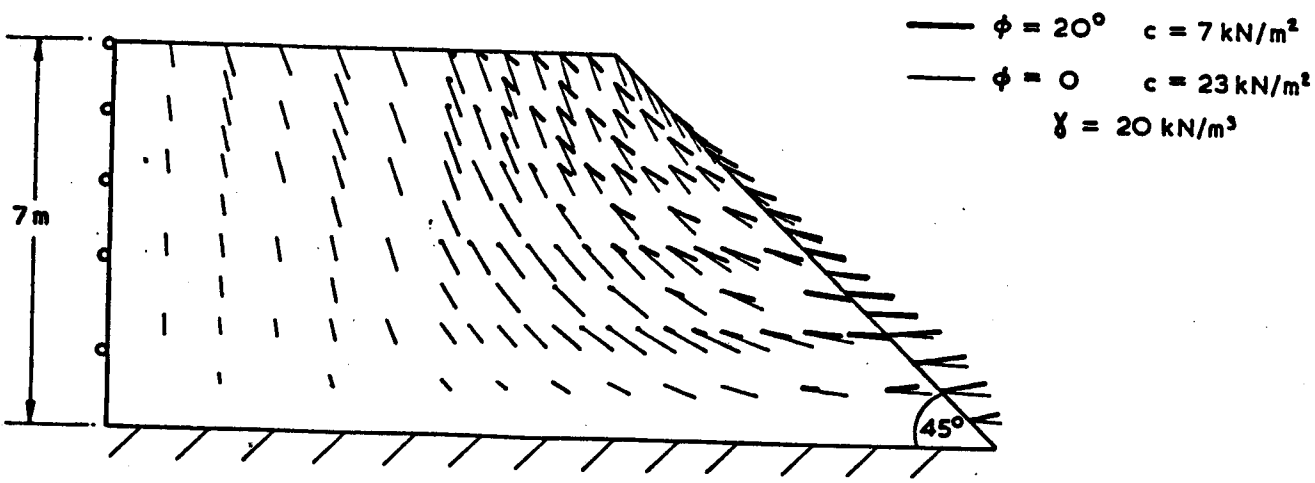

DISPLACEMENT VECTORS AT COLLAPSE

FIG. 28.

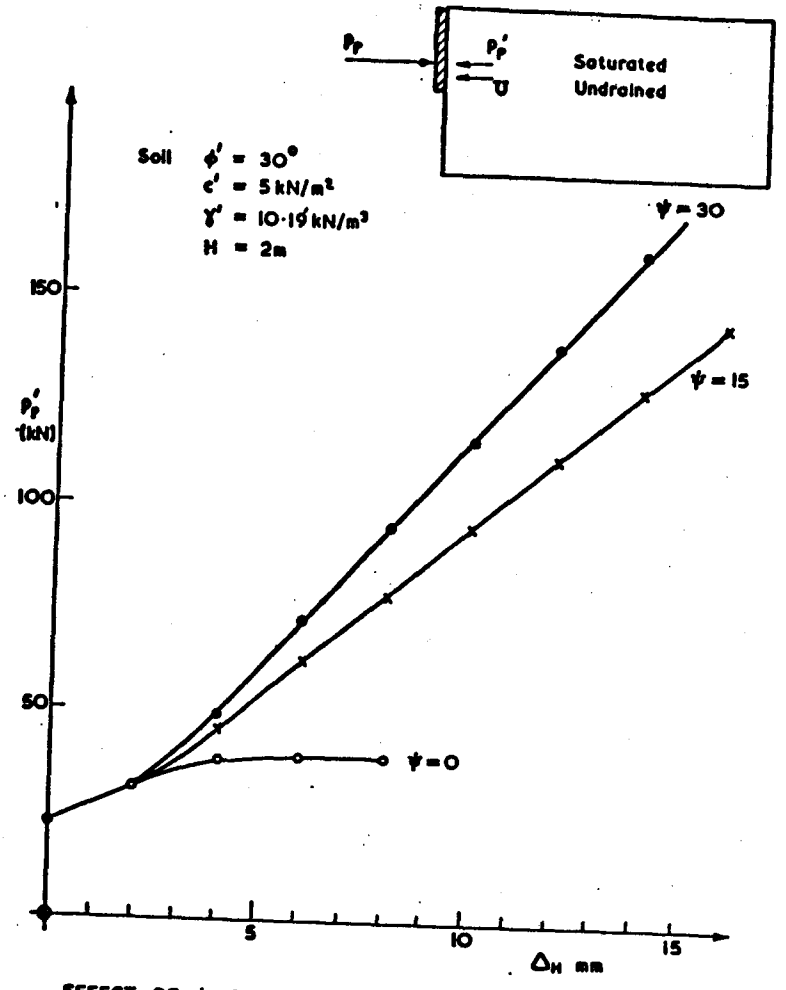

EFFECT OF ψ ON EFFECTIVE PASSIVE RESISTANCE

FIG. 29

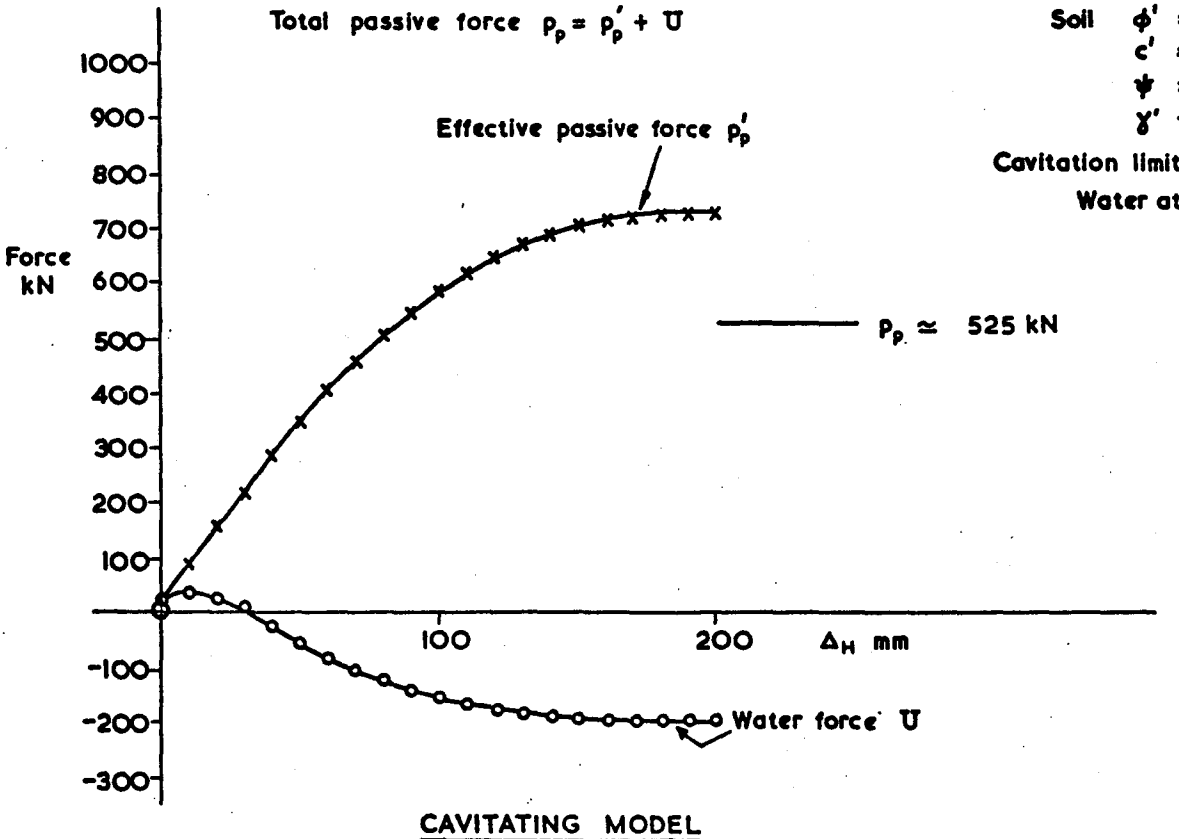

CAVITATING MODEL

FIG. 30

REFERENCES

BISHOP, A W (1966) 'The strength of soils as engineering materials', *Geotechnique*, 16 (2)

BISHOP, A W and MORGENSTERN, N R (1960) 'Stability coefficients for earth slopes', *Geotechnique*, 10 (4)

CHEN, W-F (1975) *'Limit Analysis and Soil Plasticity'*, Elsevier Scientific Publishing Company

CORMEAU, I C (1975) 'Numerical stability in quasi-static elasto/visco-plasticity', *Int. J. Num. Meth. Eng.*, 9

DUNCAN, J M and CHANG, C-Y (1970) 'Non-linear analysis of stess and strain in soils', *JSFMD, ASCE*, 96 (SM5)

KO, H-Y and SCOTT, R F (1973) 'Bearing capacities by plasticity theory', *JSFMD, ASCE*, 99 (SM1)

LADE, P V (1972) *'The Stress-Strain and Strength Characteristics of Cohesionless Soils*, Thesis presented to the University of California, Berkeley, in partial fulfilment of the requirements for the Degree of Doctor of Philosophy

MEYERHOF, G G (1951) "The ultimate bearing capacity of foundations', *Geotechnique*, 2 (4)

NAYLOR, D J (1974) 'Stresses in nearly incompressible materials by finite elements with application to the calculation of excess pore pressures', *Int. J. Num. Meth. Eng.*, 8

ROWE, P W and PEAKER, K (1965) 'Passive earth pressure measurements', *Geotechnique*, 15 (1)

SEED, H B and LEE, K L (1967) 'Undrained strength characteristics of cohesionless soils', *JSMFD, ASCE*, 93 (SM6)

SMITH, I M and HOBBS, R (1974) "Finite element analysis of centrifuged and built-up slopes', *Geotechnique*, 24 (4)

TAYLOR, D W (1937) 'Stability of earth slopes', *J. Boston Soc. Civ. Eng.*, 24 (3)

ZIENKIEWICZ, O C and CORMEAU, I C (1972) 'Visco-plasticity solution by finite element process', *Arch. Mech.*, 24

ZIENKIEWICZ, O C and CORMEAU, I C (1974) 'Visco-plasticity - plasticity and creep in elastic solids - a unified numerical approach', *Int. J. Num. Meth. Eng.*, 8

ZIENKIEWICZ, O C, HUMPHESON, C and LEWIS, R W (1975) 'Associated and non-associated visco-plasticity and plasticity in soil mechanics', *Geotechnique*, 24 (4)

ZIENKIEWICZ, O C, NORRIS, V A, WINNICKI, L A, NAYLOR, D J and LEWIS, R W (1978) 'A unified approach to the soil mechanics problems of offshore foundations', in *'Numerical Methods in Offshore Engineering'*, Wiley